

PRELIMINARY SEISMIC VULNERABILITY ASSESSMENT OF PRE-CODE MULTI-GIRDER BRIDGES IN HUNGARY

József SIMON¹ and László Gergely Vigh²

Abstract: In lack of seismic provisions in the pre-Eurocode ages, most of the existing Hungarian bridges are not designed for seismic actions. It is questioned whether they are able to retain their structural integrity after a considerable seismic event or may suffer significant damages. Based on the evaluation of a governmental bridge database, ten typical bridge types could be distinguished, covering 85% of the total amount of about 3200 bridges of higher level roads. In present study only prestressed multi-girder bridges are investigated. First, multi modal response spectrum analysis is used for parametric studies to determine critical components and layouts. Nonlinear response history along with multiple stripes analysis are also carried out for bridges sampled by Latin Hypercube method. Fragility curves of each critical component, furthermore the reliability of the selected critical bridges are determined. The analyses show that brittle shear failure of piers may occur in the case of longer bridges, the relatively high flexural ductility of the members cannot be utilized. Using fibre reinforced polymers can be a possible retrofit method, however higher reliability can be achieved in exchange of increased costs applying concrete overlay or steel jacket.

Introduction

Experiences on existing bridges (e.g. Simon and Vigh 2015), and parametric study on typical continuous girder bridges in Hungary (Zsarnóczay et al. 2014) indicate that large portions of girder bridges may be vulnerable to earthquake loads even in moderate seismic regions. Specific components such as piers, foundations and bearings may suffer severe damage. This high vulnerability stems from: a) prior to the European structural codes – Eurocode 8 Part 1 and Part 2 (EC8-1, EC8-2) (CEN 2006, CEN 2008) –, bridges in Hungary were conventionally designed with no or minimal consideration of seismic loads; b) in 2006 a new seismic hazard map (Tóth et al. 2006) was released with an increased seismic proneness, classifying Hungary as moderate seismic zone. Evaluation of a national road bridge database (KKK 2014) shows that the number of prestressed multi-girder (PMG) bridges counts for nearly half of the ~3200 bridges of higher level roads (Fig.1), therefore the first goal of the research is to determine the seismic vulnerability of these bridges.



Figure 1. Selected bridges for seismic performance evaluation on higher level roads. PMG bridges are marked with black dots.

For preliminary calculations parametric multi modal response spectrum analysis (MMRSA) is carried out according to EC8-2. Critical layouts and components are determined, a rough estimation of critical bridges is provided based on the MMRSA results. As a next step,

¹ PhD Student, Budapest University of Technology and Economics, Department of Structural Engineering, Budapest, simon.jozsef@epito.bme.hu

² Associate Professor, Budapest University of Technology and Economics, Department of Structural Engineering, Budapest, vigh.l.gergely@epito.bme.hu

representative bridges are sampled with the Latin Hypercube technique, multi stripes analysis (MSA) is carried out to predict the probability of different damage states and assess the risk associated with them.

Description of multi-girder bridges

PMG bridges are most widely used as overpass bridges on highways, but they are also built as highway bridges in multi-span system. They are constructed by placing a number of prestressed beams on the piers and on the abutments, adjacent to one another, then with reinforcing bars and freshly poured concrete a quasi-slab system is created. This is beneficial since there is no need for expensive stand and formwork construction. Fig.1a depicts the general layout of PMG bridges. According to the Hungarian practice, PMG bridges with a few exceptions are built as continuous systems instead of simple supported ones. The connection between the superstructure (SS) and the substructure (SBS) is constructed with vertical bars (ϕ 16/300- ϕ 20/300) to transfer lateral loads (Fig.1b). The structural height of the SS is determined as the function of the span length by analysing existing bridges considering an equivalent slab taking into account stiffness and mass properties.

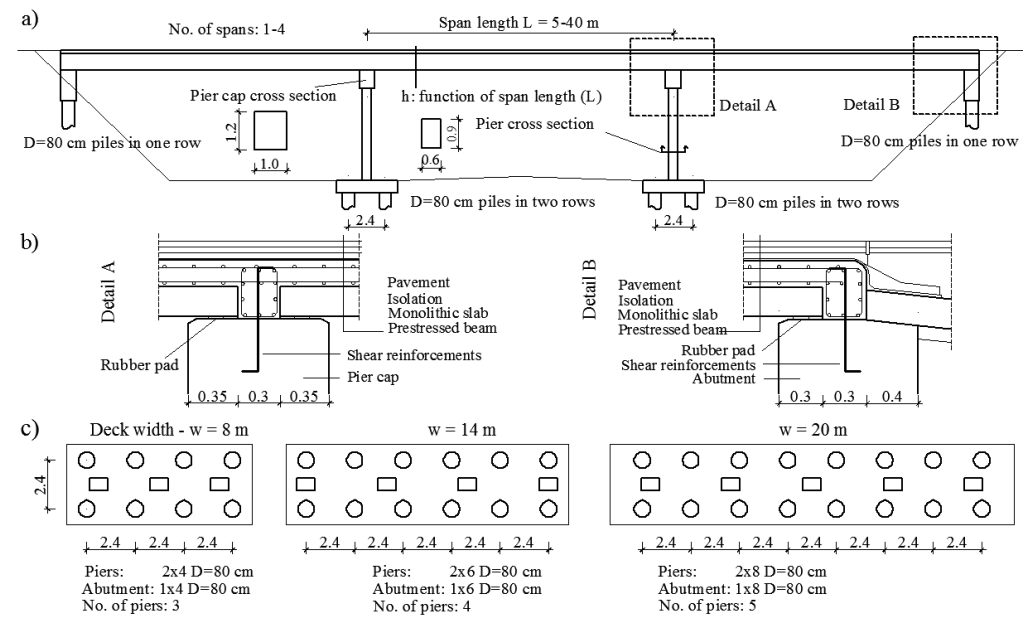


Figure 1. General layout of PMG bridges: a) side-view of the bridge; b) details of the SS-SBS connection; c) applied pile foundation arrangements for different bridge widths.

The piers are generally constructed as multi-column bents. Since these bridges are commonly used as overpass bridges on higher level roads, cross section of the piers (0.6 m x 0.9 m) and the pier cap (1.0 m x 1.2 m) and the dimensions of the abutments (1.0 m x 2.0 m) are more or less the same for all structures for the sake of the efficient reusability of formwork. Longitudinal reinforcement ratio is usually around 0.007-0.010, while minimal shear reinforcement (mostly \$\phi12/250-300\$) is applied due to the low shear forces in conventional design situations. The distance of the piers are generally 3-4 m in the transverse direction. The foundation system is pile foundation in most of the cases, the layouts for different deck widths are shown in Fig.1c. The input parameters for parametric analysis are determined with the help of statistical analysis of the bridge database (KKK 2014). In Fig.2a-d, nonparametric probability mass function for the number of spans, deck width, pier height and span length is depicted, respectively. Variable and fixed parameters are: number of supports (2-5), span of single bay (5-30 m), deck width (8, 14 and 20 m) and pier height (2-10 m). For simplifications, pier and pier cap cross-section, height of the SS, abutment geometry and layout of the pile foundation are considered fixed or the function of the variable parameters during the studies.

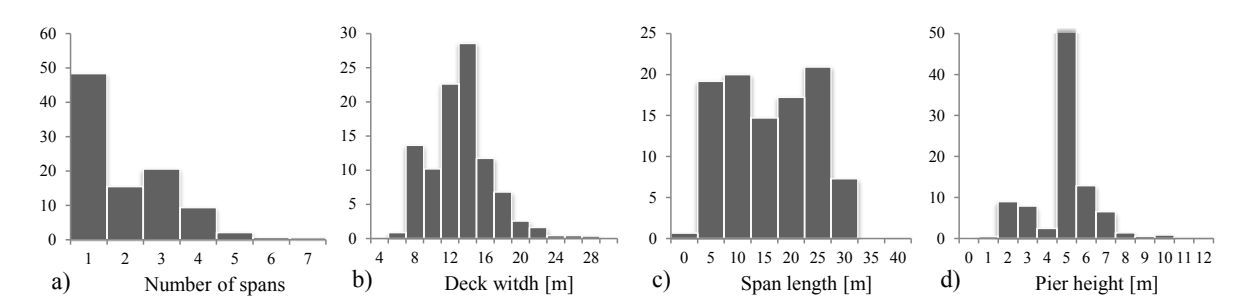


Figure 2. Statistical evaluation of the database, non-parametric probability mass function (%) for the number of spans (a); the deck width (b); pier height (c) and span length (d).

Analytical model and applied analysis methods

A three dimensional beam-element model shown in Fig.3 is created in OpenSees finite element software environment (McKenna et al. 2010). The beam elements are placed in the center of gravity, and eccentricity between the member axes is bridged over by the help of rigid elements. The connections between the SS and the SBS are modelled by zero-length elements with linear spring characteristics of 10¹³ N/m to model fully rigid connections. The soil-structure interaction (SSI) at the foundations is taken into consideration with integrate linear springs (ranging from 10⁹ to 5·10¹⁰ N/m and Nm/rad values for translational and rotational stiffness). Pile layouts for different deck widths can be seen in Fig.2c. The backfill soil under compression provides extra support at the abutments due to the developing passive earth pressure. This behaviour is incorporated in the model with the help of linear springs. Since this behaviour occurs only under compression, during linear MMRSA this can be taken account by applying these springs at one abutment only. The stiffness of the linear springs are calculated according to Caltrans (2013).

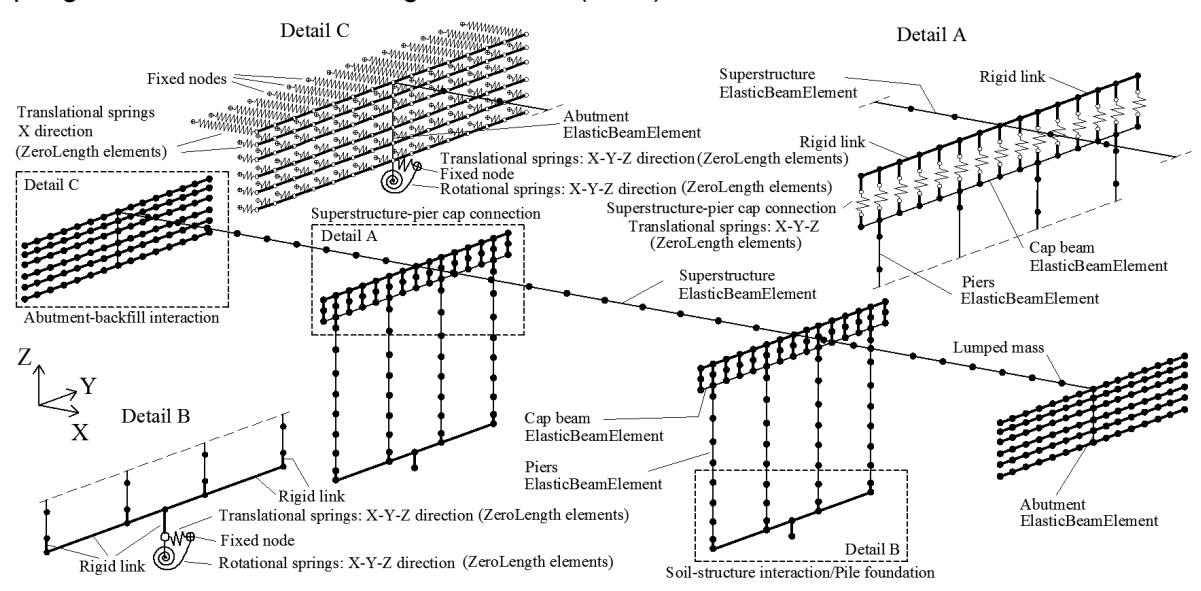


Figure 3. Beam element model in OpenSees.

Parametric study using MMRSA

An OpenSees procedure is written by the authors (Simon and Vigh 2014) in TCL language to carry out MMRSA in accordance with EC8-1 and EC8-2. The parameters of the standard acceleration response spectrum (EC8-1) curve (a_g =1.5 m/s², soil type D, M>5.5, ξ =0.05) with a return period of 475 years are defined in a way to obtain conservative results. The modal analysis results (Fig.4) show the high stiffness and thus low natural periods of these structures. This indicates that high base shear forces are expected as a result of the MMRSA.

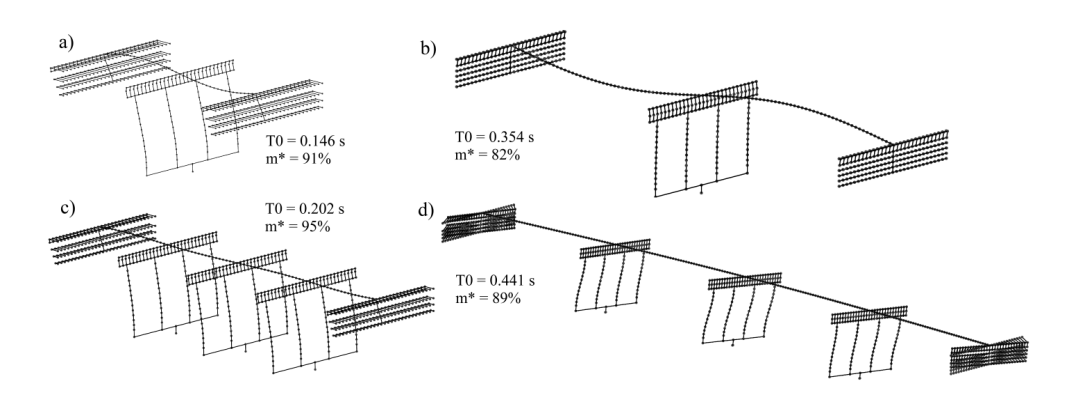


Figure 4. First eigenshapes and natural periods for different typical layouts.

Although SSI is taken into account in a simplified way, three cases are examined to consider different soil conditions. In each case one SSI is considered to be stiffer (the backfill soil, the abutment foundation or the pier foundation) than the other two, then the analyses are carried out to obtain conservative results for each component. For brevity, results from MMRSA are presented in Fig.5 only for the most critical component: the pier in case of three span bridges. Demands are higher in the transverse direction that stems from the half-integrated construction, high stiffness of the abutment and backfill soil supporting the structure in the longitudinal direction. Seismic demands of a typical overpass bridge (14 m width, 5 m pier height) are: $F_x = 450 \text{ kN}$, $F_y = 650 \text{ kN}$, $M_x = 1500 \text{ kNm}$, $M_y = 550 \text{ kNm}$. This implies that in contrary of simple girder bridges, the transverse direction may be the critical one regarding the seismic action, especially with higher piers.

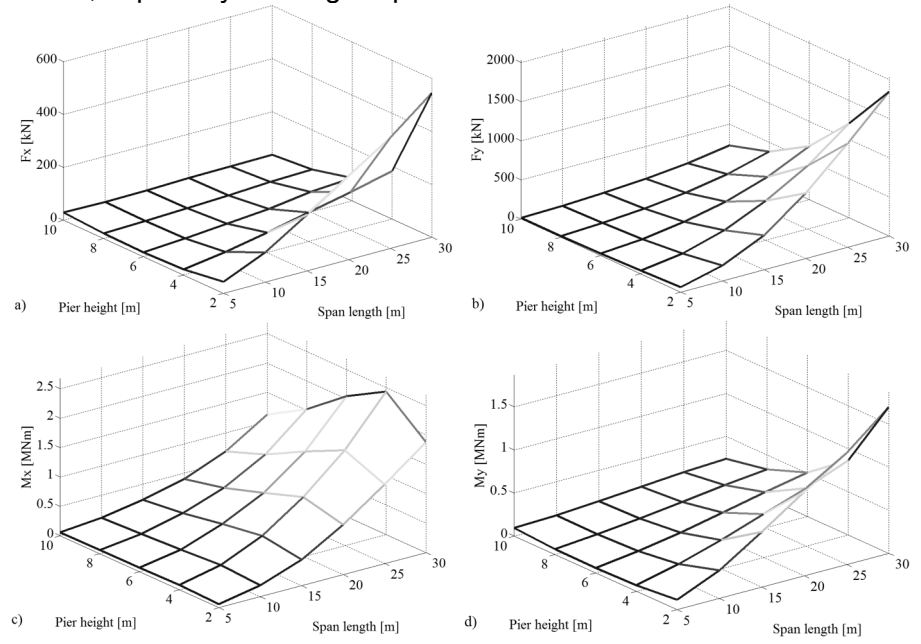


Figure 5. Pier internal forces: a) F_x - longitudinal shear; b) F_y - transverse shear; c) M_x - transverse bending moment; d) M_y - longitudinal bending moment.

Further results for a regular highway overpass bridge is presented to show the order of magnitude of the demands. The SS demands are slightly above the ones of ultimate limit state (ULS) indicating possible failure which is rarely observed at continuous girder bridges. Typical SS-SBS joint shear forces for the entire width are: F_x = 10500 kN, F_y = 6500 kN at the abutment, and F_y = 9500 kN at the pier, while the longitudinal shear force F_x can be neglected (only 550 kN). Pile normal forces can be used to estimate whether compressive resistance failure occurs or not. Pile forces are: F_p = 1900 kN at the abutment and F_p = 2250 kN at the pier. The abutments are considered as solid blocks, thus demands are determined

as the maximum longitudinal displacement that can possibly cause stability failure, while the backfill soil demands are measured with the maximum passive earth pressure. Seismic demands of a regular bridge are: σ = 120 kPa and d_x = 13 mm. The results indicate that it is unlikely that these components are critical, the pressure never reaches 350 kPa (failure threshold proposed by Caltrans), while the displacements are always under 30 mm (which is a rational displacement capacity in case of seat type abutments with 2 m height as it is proposed by EC8-2).

Critical components and layouts

The above-presented demands are calculated considering the highest peak ground acceleration (PGA) value of 1.5 m/s² in Hungary to give an estimated upper-limit. In order to determine critical components and layouts, capacities of each component should be defined. These capacities are calculated in accordance with standard formulae (EC8-2) or an assumed load bearing capacity is used (e.g. the SS should withstand the demands lower than those in ULS). Instead of presenting demand capacity ratios (D/C) which would represent only one PGA level, maximum acceptable PGA (MAPGA) is calculated by dividing the currently applied PGA with the D/C ratio. The bridges are assumed to collapse if one of the components fail (assumed simple series system), therefore it is important to understand which component is the most vulnerable for different layouts. In Fig.6 MAPGA results for three-span bridges with 14 m width are depicted. The abbreviations are: SS (SS ULS); joints (B1, B2), where 1 and 2 denote abutment and pier, respectively; foundations (F1, F2); pier bending (PM); pier shear (PV). For smaller span lengths SS tends to be the most vulnerable, while at longer spans shear failure of short piers or bending failure of high piers are dominant. The pile foundation and the pier joint are less vulnerable, failure of the SS or the piers are far more possible. It should be noted, however, that these conclusions are drawn from results calculated with a behaviour factor of 1.0. Both SS and piers may have at least a limited ductility of 1.5. This emphasizes the high vulnerability of piers against brittle shear failure.

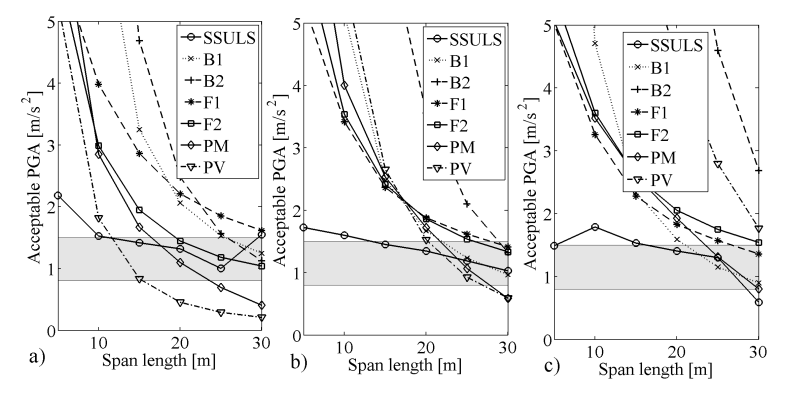


Figure 6. MPGA values for three-span bridges: a) 2 m; b) 6 m and; c) 10 m pier height and 14 m deck width. PGA values in Hungary are marked with shaded area.

Estimation of the number of critical PMG bridges in Hungary

Evaluation of the seismic performance of PMG bridges is carried out applying interpolation on the MAPGA values. Essential parameters are the number of spans, deck width, pier height and span length. Evaluation of bridges with missing parameters are excluded. The bridge database also contains the coordinates of each bridge. Possible failure of each component is calculated comparing the PGA value according to the seismic zone map of Hungary and the MAPGA obtained by interpolation for the actual bridge. The MAPGA value is modified with a factor reflecting bridge condition which is rated with a 5 level scale in the database with 1 being excellent condition and 5 being extensive damages. From condition 1 to 5 a factor of 1.0, 0.9, 0.8, 0.7, 0.6 is applied, respectively. There are 1300 bridges with span length over 5 m and 1030 bridges have the data required for interpolation (615 single span and 415 multi-span bridges). 13% of the single-span bridges will possibly suffer SS

failure, however the D/C ratios are just slightly over 1.0 in most of the cases (not considering the limited ductility of 1.5). The number of possibly failing components normalized by the total number of multi-span bridges is presented in % in Fig.7a. The high vulnerability of the SS and of the piers for shear is confirmed, for nearly 60% of the bridges SS is a critical component, while over 50% of the bridges may suffer pier shear failure. Pier bending failure can occur for nearly 30% of the bridges, while there is a possibility of joint shear failure in case of over 10% of the total number of bridges. Lower vulnerability of the pier joint and pile foundations are also confirmed. These components may belong to different layouts, however one critical component is enough to consider the whole bridge vulnerable. Observing all the bridges (including single span bridges as well) 37% of the bridges have a critical component (which is mostly pier shear failure) and are considered vulnerable against a seismic event even in a moderate seismic zone like Hungary due to the lack of seismic design.

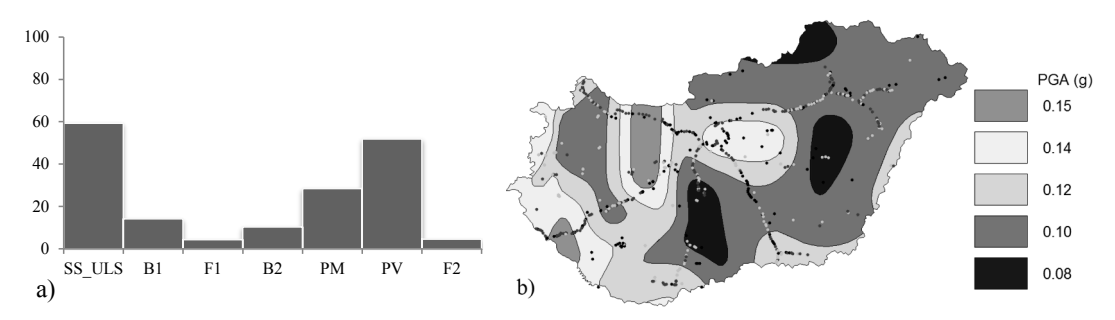


Figure 7. a) Critical bridge component of multi-span bridges in % of the total bridge number. b) Bridges with possible pier shear failure (black dots) in the seismic zone map of Hungary.

In Fig.7b bridges with possible pier shear failure are plotted with black dots, while adequate bridges are marked with green in the seismic zone map of Hungary. The high vulnerability against shear forces caused by an earthquake is highlighted, failure occurs even in lower seismic areas. These maps are useful tools to identify bridges with the possibility of failure and to select regions of interest for a possible retrofitting project. The results are not sufficient to estimate damages, but they sketch the most vulnerable components, critical bridges can be selected and their locations can be determined.

As a next step, Latin Hypercube (LHC) sampling method is applied to choose representative structures (Table 1) which are most likely present on highways. The numerical model is updated with nonlinear elements and material models for higher level nonlinear response history analysis (NRHA). Fragility analysis is carried out to determine the probability of occurrence of different damage levels/limit states, then hazard curve obtained from the European Facility for Earthquake Hazard and Risk website (EFEHR, http://www.efehr.org/) for a specific Hungarian site is used to estimate the risk of different damages or collapse in a predefined time window. This procedure is explained in the following sections.

Tabl	le 1. Bri	dges	sample	d with	the LI	HC me	ethod	(width,	span	length	and p	ier he	ight ar	e in m).
Bridge #	1	2	3	4	5	6	7	8	9	10	11	12	13	14	
No. Spans	2	3	3	2	2	3	3	3	4	3	2	3	3	3	
Width	14.2	15.2	13.4	9.2	16.2	14.4	14.0	13.6	13.7	12.0	12.2	8.6	15.9	8.2	1

Bridge #	1	2	3	4	5	6	7	8	9	10	11	12	13	14	15
No. Spans	2	3	3	2	2	3	3	3	4	3	2	3	3	3	4
Width	14.2	15.2	13.4	9.2	16.2	14.4	14.0	13.6	13.7	12.0	12.2	8.6	15.9	8.2	17.6
Span length	17.0	8.0	27.6	22.4	25.4	22.0	18.6	10.0	9.7	13.4	24.3	18.4	31.0	24.4	30.0
Pier height	3.0	3.0	4.6	4.7	4.7	4.7	4.7	4.7	4.7	4.7	4.8	4.8	4.8	4.9	4.9
Bridge #	16	17	18	19	20	21	22	23	24	25	26	27	28	29	30
No. Spans	2	4	4	3	2	2	3	4	4	2	2	3	2	3	3
Width	8.6	8.2	8.1	10.1	12.7	6.2	12.1	27.7	19.0	12.0	8.6	14.8	15.4	10.8	8.0
Span length	21.8	14.4	25.0	15.0	22.8	19.9	14.0	20.8	24.2	26.2	23.0	11.6	16.4	24.0	20.4
Pier height	5.0	5.0	5.0	5.1	5.2	5.4	5.6	5.7	5.9	6.2	6.5	6.7	7.5	8.0	9.0

6

Adopted fragility analysis procedure

Seismic performance can be assessed based on fragility curves which are conditional probability statements (P(LS|IM)) giving the probability of a bridge reaching or exceeding a particular limit state (LS) for an earthquake of a given intensity measure (IM) level. An estimated fragility function can also be combined with a seismic hazard curve ($\lambda(IM)$) to compute the mean annual rate of structural collapse (or reaching the given damage state):

$$p_{collapse} = \int_{IM} P(LS_{collapse}|IM = im) d\lambda (IM = im), \tag{1}$$

This is beneficial since the risk of a LS occurrence in a predefined time-window can be determined, retrofit decisions can be made regarding economical and financial aspects. The fragility function is usually estimated with a lognormal (LN) cumulative distribution function (CDF), widely applied methods exist such as Incremental Dynamic Analysis (IDA) (Vamvatsikos and Cornell 2002) and Multiple Stripes Analysis (MSA) (Jalayer and Cornell 2009). In this study MSA method is adopted since it is proved to be more efficient (Baker 2015) fragility estimates than IDA for a given number of structural analyses, provided that some knowledge of the bridge capacity is available prior to the analysis so that relevant portions of the fragility curve can be approximately identified. 13 intensity levels are selected for each examined bridge based on the results of the MMRSA. PGA is selected as the optimal IM in this study for three reasons: 1) in the study of (Nielson 2005) it is shown that PGA well represents the demands of continuous PMG bridges; 2) PGA is compatible with the hazard curves used in this study; 3) comparison between fragility curves are far more easier with a general IM such as PGA. MSA has other benefits compared to IDA, it allows for different ground motions to be used at varying intensity levels, to represent the differing characteristics of low and high intensity shaking. However at current state there is no information (deaggregation is not yet provided at the EFEHR website) about the dominant seismic characteristics (magnitudes, rupture distances etc.) which contribute most to the chosen 13 intensity levels which is important for ground motion selection procedures. Thus, preliminary fragility analysis is carried out with artificial motions (such as in a recent study of Borzi et al. 2015) which are generated to match standard spectrum provided by EC8-1.

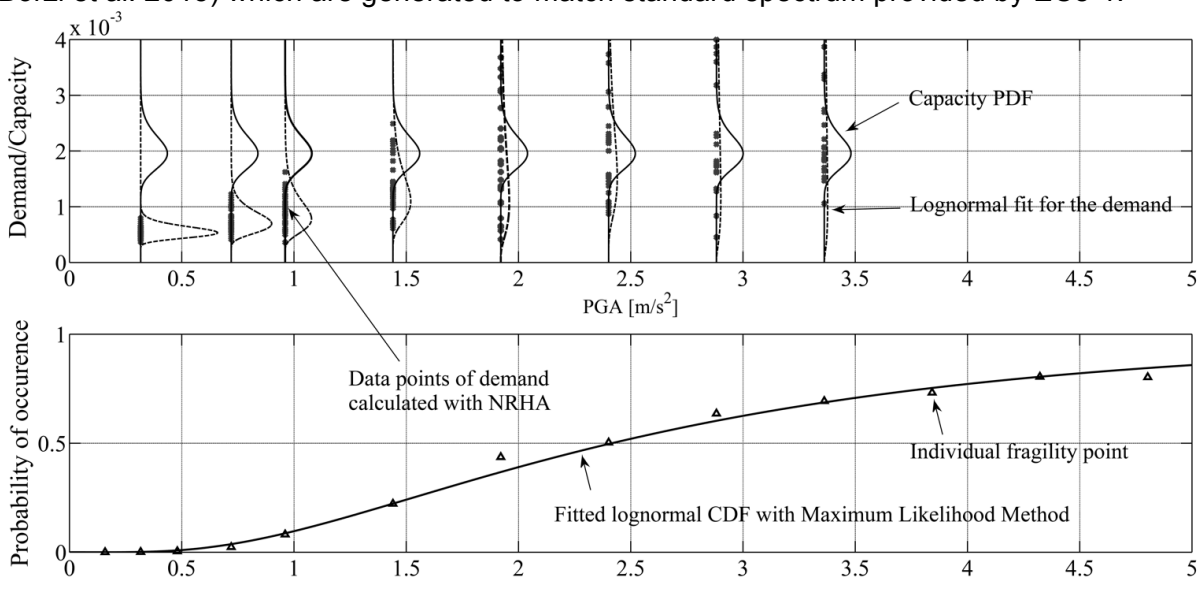


Figure 8. MSA procedure.

The MSA procedure is explained in Fig.8. At each intensity level 30 artificial ground motions are generated in both horizontal directions. Demands are registered during NRHA, then assuming LN distribution the median and the coefficient of variation (CoV) is determined for the demands. A single fragility point at an intensity level is obtained as follows:

$$P[(D > C_{LS})|IM] = \int_0^\infty P(D > \alpha |IM) P(C_{LS} = \alpha) d\alpha, \tag{2}$$

where the second function is the PDF of the capacity and α denotes integrating over the demand parameter. As a last step maximum likelihood method is applied to obtain the fitted LN CDF estimation of the fragility function with a method proposed by Baker (2015). Once the fragility function is obtained, risk can be computed with Eq.(1), then the reliability index (β) can be determined with the inverse standard normal CDF: $\beta = -\phi^{-1}(p_{collapse})$.

Updated numerical model

The numerical model is updated for the NRHA. Based on the results of the MMRSA piers are the most critical components, thus fragility analysis is carried out focusing on the damage states of this component only. Piers now are modelled with nonlinear beam elements, material nonlinearity is taken into account with the help of fibre sections, while geometric nonlinearity is incorporated by modelling second order effects ($P-\Delta$). Concrete01 (OpenSees) along with Steel01 material models are used to model the unconfined, confined concrete and reinforcing bars. Confined concrete properties are calculated in accordance with EC8-2 Annex E, however it should be emphasized that due to the low shear reinforcement ratio (\sim 0.0012), the increase of strength and ductility of the confined concrete is insignificant (<5%). Other components such as the backfill soil or the SS-SBS joint could be updated with nonlinear cyclic material models as well, however regarding the piers it would result a less conservative estimate of the demands. The lower secant stiffness of the backfill soil system lets the whole SS move in the longitudinal direction and the rigid joint transfers the shear forces to the piers caused by this movement.

Capacity thresholds and uncertainties

Three flexural limit states according to Priestley et al. (1996) are considered: serviceability (PM1), damage control (PM2), and survival or collapse limit states (PM3) (Table 2). This approach is in line with Eurocode concepts. The thresholds are determined through moment-curvature analysis of the pier cross-sections. Since spatial analysis is applied, the LS thresholds are expressed in steel or concrete strains, instead of checking displacement or curvature ductility in each direction. The defined thresholds belong to the first yield of the steel (ϵ_{sy}), spalling of concrete (ϵ_{c}) and ultimate strain of the external concrete fiber (ϵ_{cu}), respectively. Because shear failure is brittle type failure mode, only collapse LS (PV) is defined. Shear capacity is calculated with the formula (Priestley et al. 1996) presented in Table 2.

Table 2. Limit states,	capacit	v thresholds and	d uncertainties	taken into	consideration.
rabio E. Ellini otatoo,	Capacit	, and our or ar a	a antoontamineo	tartori irreo	oonioidoi dilioin.

Limit	states and capacity	thresholds LND	Other inputs with uniform distribution					
LS	Mechanism	Median	CoV	Parameter	Min.	Max.		
1 - PM1	Flexure	$\epsilon_{\rm sy}$	0.30	Steel Young modulus	195 GPa	205 GPa		
2 - PM2	Flexure	$\epsilon_{ m c}$	0.35	Long. reinf. ratio	0.007	0.010		
3 - PM3	Flexure	ϵ_{cu}	0.40	Pier cross section - a	0.58 m	0.62 m		
1 - PV	Shear	$V_{u} = V_{c} + V_{N} + V_{s}$	0.25	Pier cross section - b	0.88 m	0.92 m		
	Input parameters L	LND		Pier height	+ 10 cm	- 10 cm		
Parameter		Median	CoV	SS mass	-10%	+10%		
Concrete streng	th	20 MPa	0.15					
Steel yield stren	igth	420 MPa	0.10					

Uncertainties are taken into account by assuming input parameters as random variables of specified distributions. Since artificial ground motions match the standard spectrum, record to record variability is taken into account by multiplying the amplitudes by a random factor assumed to have a LN distribution with a mean value of one and a CoV of 0.5. Uncertainties in the capacity and material properties are also taken into consideration along with other input parameters (Table 2). For instance, the median of the concrete compressive strength is set to 20 MPa with a CoV of 0.15, while the median yield strength of the reinforcing steel is 420 MPa with a 0.1 CoV assuming LN distribution.

Results of the fragility analysis

Fragility curves of Bridge #6 (a typical three span highway bridge) from Table 1 can be seen in Fig.9a. It is obvious that the shear failure is dominant, it possibly occurs before the first yielding of the section. According to the moment-curvature analysis, the sections can have curvature ductility up to 4-5, however this ductile behaviour cannot develop due to the possible brittle failure caused by shear forces. Fragility curves for shear failure are shown in Fig.9b for all the bridge samples. Median values of the LN CDF fragility function are ranging from 0.31 to over 3.0 g, which confirms the findings of Borzi et al. (2015) that the fragility function highly depends on the actual layout and simple classification of bridges into few bridge classes does not provide reliable results.

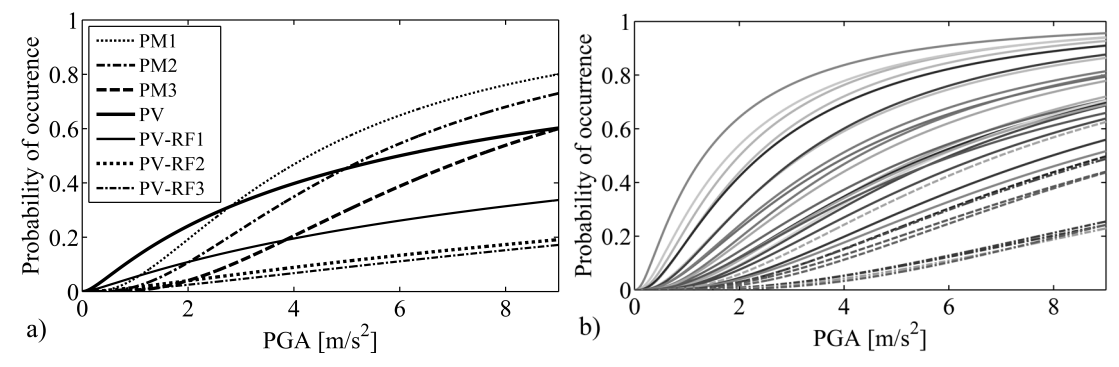


Figure 9. Fragility curves: a) for each component (Bridge #6) and for shear failure after retrofit; b) for shear failure (all bridges) (dashed line: $\beta > \beta_B$; dash-dot line: $\beta > \beta_C$).

The β index is calculated for all the bridges (Fig.10) for each LS along with the target values proposed by JCSS (2001) considering moderate consequences of failure and large (β_A), normal (β_B) and small (β_C) relative costs of safety measure. The hazard curve for a 50 year time window applied for the calculations is the one for Komárom which is the area of highest seismicity in Hungary with PGA = 0.15 g (return period of 475 years). In all cases, β associated with shear failure is the lowest indicating similar behaviour presented in Fig.9a confirming the MMRSA results, that large portion of the bridges are highly vulnerable against shear forces. β values for shear failure are ranging from 0.8-2.5, even the basic criteria of 1.98 is not always met (>85%), without any seismic design the lowest target index can be reached only in case of shorter bridges (<50 m). Flexural failure reliabilities are higher (ranging 1.1-3.5), however more than 20% of the bridges are not adequate considering the lowest target β value. This indicates that higher reliability should be and can be reached with retrofit methods for longer and even for shorter bridges.

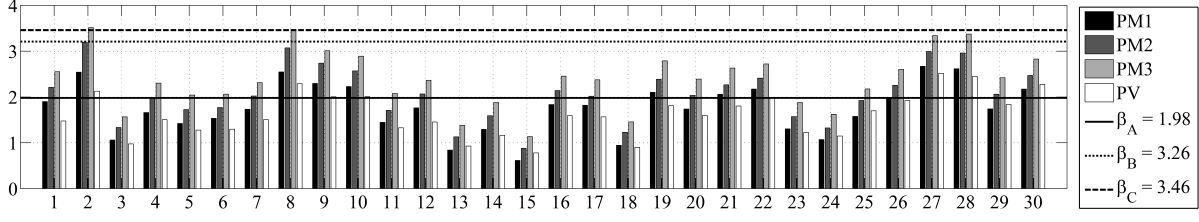


Figure 10. Calculated β reliability indices and target indices according to JCSS (2001).

Possible retrofit methods and concluding remarks

Fragility curves confirm that flexural behaviour is mostly sufficient, but shear capacity shall be improved. Using FRPs may be economical solution, besides the total cost is relatively low and the construction is simple in comparison to other retrofit techniques such as steel jacket or concrete overlay. The latter methods have the benefit of increasing the flexural capacity and ductility, which may be needed for critical bridges regarding flexural failure. In Fig.9a fragility curves from three retrofit methods (RF1-RF3) are also indicated: an increase of shear resistance (\sim 600 kN) by a factor of 2.5 (PV-RF1), 3.5 (PV-RF2) and 4.0 (PV-RF3) is assumed in the three cases. The resulting β values are 2.05, 2.16, 2.34 respectively. The

first method is manageable with FRP, however higher reliability can be only reached with the two other methods which can cost significantly more. The D/C ratio for shear failure calculated from MMRSA is 2.58 which corresponds to the first retrofit version. This indicates that retrofit design according to MMRSA would lead to the minimal target reliability and in this case it is enough to match the flexural and shear failure collapse risk and to fully utilize the flexural ductility.

The presented results well illustrate the efficiency of MMRSA in determining the critical components and layouts. It also provides prior knowledge on the expected intensities associated with limit states, which can be utilized during MSA. Fragility and risk analysis show that these bridges are highly vulnerable to shear failure, however flexural behaviour is sufficient in most cases. A possible retrofit method using FRP can increase the reliability and sufficient seismic performance criteria can be met, however higher reliability can be reached with less cost-effective methods only. Proper selection of retrofit strategies shall be based on economic and financial judgments.

ACKNOWLEDGEMENT

This paper was supported by the János Bolyai Research Scholarship of the Hungarian Academy of Sciences.

REFERENCES

Baker JW (2015) Efficient analytical fragility function fitting using dynamic structural analysis, Earthquake Spectra 31(1) 579-599.

Borzi B, Ceresa P, Franchin P, Noto F, Calvi GM and Pinto PE (2015) Seismic Vulnerability of the Italian Roadway bridge stock, Earthquake Spectra, (in press).

Caltrans (2013) Caltrans Seismic Design Criteria, California Department of Transportation, Sacramento, CA, Version 1.7.

CEN (2006) EN 1998-2:2006 Eurocode 8: Design of structures for earthquake resistance-Part 2, CEN

CEN (2008) EN 1998-1:2008 Eurocode 8: Design of structures for earthquake resistance-Part 1, CEN

EFEHR (2015) European Facility for Earthquake Hazard and Risk website (http://www.efehr.org/)

Jalayer F and Cornell CA (2009) Alternative nonlinear demand estimation methods for probability-based seismic assessments, Earthquake Engineering & Structural Dynamics, 38: 951-972.

JCSS (2001) Probabilistic model code – Part 1: Basis of design, JCSS.

KKK (2014) *Integrated Bridge Database (Egységes Hídnyilvántartási Rendszer)*. Hungarian Transport Administration. (http://www.hidadatok.hu)

McKenna F, Feneves GL (2012) *Open system for earthquake engineering simulation*, Pacific earthquake engineering research center, version 2.3.2.

Nielson BG (2005) *Analytical Fragility Curves for Highway Bridges in Moderate Seismic Zones*, PhD dissertation, School of Civil and Environmental Engineering, Georgia Institute of Technology.

Priestley MJN, Seible F and Calvi GM (1996) Seismic Design and Retrofit of Bridges, John Wiley & Sons, Inc., New York, NY.

Simon J, Vigh LG (2014) *Multi modal response spectrum analysis implemented in OpenSEES,* In: OpenSees Days Portugal 2014, Porto, 03-04 July, pp. 39-42.

Simon J and Vigh LG (2015) Application and assessment of equivalent linear analysis method for conceptual seismic retrofit design of Háros M0 highway bridge, Periodica Polytechnica, (in press).

Tóth L, Győri E, Mónus P, Zsíros T (2006) *Seismic Hazard in the Pannonian Region*, The Adria Microplate: GPS Geodesy, Tectonics, and Hazards, Springer Verlag, NATO ARW Series 61, 369-84.

Vamvatsikos D and Cornell CA (2002) *Incremental Dynamic Analysis*. Earthquake Engineering & Structural Dynamics 31:491–514.

Zsarnóczay Á, Vigh LG, Kollár LP (2014) Seismic Performance of Conventional Girder Bridges in Moderate Seismic Regions, Journal of Bridge Engineering 19(5), 9 p. Paper 04014001.